Core Expansion and Electronic Structure of the Porphyrin in the Neutral pH Form of Copper Cytochrome c

ARTICLE *in* BIOCHEMISTRY · AUGUST 1984

Impact Factor: 3.02 · DOI: 10.1021/bi00312a023

5 AUTHORS, INCLUDING:

John A Shelnutt
University of Georgia
265 PUBLICATIONS **8,849** CITATIONS
SEE PROFILE

David Straub
University of Arkansas for Medical Sciences
103 PUBLICATIONS **1,320** CITATIONS
SEE PROFILE

Peter M Rentzepis
University of California, Irvine
379 PUBLICATIONS **10,021** CITATIONS
SEE PROFILE

Core Expansion and Electronic Structure of the Porphyrin in the Neutral pH Form of Copper Cytochrome *c*†

J. A. Shelnutt,* K. D. Straub, P. M. Rentzepis, M. Gouterman, and E. R. Davidson

ABSTRACT: The pH-dependent resonance Raman and absorption spectra of copper cytochrome *c* are examined. Large shifts in the Raman core-size marker lines are observed in the neutral pH form of copper cytochrome *c* relative to the protein at pH extremes (pH 2 and 13). The 5-coordinate copper–porphyrin complexes exhibit similar, but somewhat smaller, shifts in the core-size marker lines. The Raman shifts represent a significant expansion (0.03 Å) of the porphinato core in the neutral form. Further, analysis of the $\pi \rightarrow \pi^*$ absorption spectral changes using the four-orbital model indicates a substantial destabilization of the top-filled $a_{2u}(\pi)$ orbital if the neutral pH form of the protein has 5-coordinate copper. The result is a red shift of all $\pi \rightarrow \pi^*$ bands, a decrease in the separation of the α-band and Soret band, and a reversal in the α- and β-band absorbance ratio from ~1.4 to ~0.8. Iterative extended Hückel molecular orbital (MO) calculations for model 4-, 5-, and 6-coordinate copper porphyrins show considerable destabilization of the a_{2u} orbital caused by addition of a σ-donating axial ligand. Thus, the calculations support previous interpretations of spectral changes based on addition of an axial fifth ligand in the copper-modified heme proteins and copper porphyrins in coordinating solvents. The MO calculations are also consistent with studies associating a_{2u} orbital energy with the frequency of Raman marker lines. They further predict an observed new, strong UV band near 350 nm in the neutral form of copper cytochrome *c* and 5-coordinate copper–porphyrin complexes to be a $d_{z^2} \rightarrow e_g(\pi^*)$ charge-transfer band. No evidence for 6-coordination of copper is found. Finally, changes in Raman and absorption spectra at the pH extremes are consistent with dimerization of the porphyrins in the copper cytochrome *c* dimers.

Recently, metal-substituted cytochromes *c* have been synthesized (Flatmark & Robinson, 1968; Turner, 1971; Dickinson & Chien, 1974) and characterized by various techniques (Findley et al., 1977; Chikira et al., 1980; Moore et al., 1980; Dixit et al., 1982; Straub & Rentzepis, 1983). The aim of this work is to further our understanding of the role of the metal ion in electron-transport hemoproteins and to elucidate the effects of the protein moiety on its coordination chemistry.

A particularly interesting metal derivative of cytochrome *c* is that with copper(II) substituted for the iron ion (Findley et al., 1977; Chikira et al., 1980; Straub & Rentzepis, 1983). At neutral pH the native "A" form of the Cu derivative (^{Cu}cyt-*c*) has an unusual Cu–porphyrin absorption spectrum (Findlay et al., 1977). In alkaline (pH 13) or acid (pH 2) solution, however, a normal Cu(II)–porphyrin spectrum is observed (Figure 1) with typical wavelengths for α- and Soret-band maxima and a normal α/β-band absorbance ratio of ~1.4. At neutral pH, however, the Cu–porphyrin spectrum is drastically red shifted and has an inverted α/β-band ratio of ~0.8.

In an effort to determine the origin of these protein-induced changes, we have obtained Raman spectra of the acid, alkaline, and neutral forms of ^{Cu}cyt-*c*, as well as model Cu–porphyrin complexes. To aid in interpreting the Raman and absorption spectral data, we have also performed molecular orbital calculations for copper(II) porphyrins and model axial ligand complexes.

Under Results, it is shown that pH-dependent spectral changes in ^{Cu}cyt-*c* are complicated by both dimerization and changes in coordination number. Nevertheless, the spectral changes indicate the Cu porphyrin in ^{Cu}cyt-*c* is dimeric and 4-coordinate at the pH extremes and monomeric and 5-coordinate at pH 7. After a brief summary of previous work on Cu-modified hemoproteins under Discussion, the Raman marker line shifts are shown to point to a significant structural modification in the porphyrin in the neutral form of ^{Cu}cyt-*c*, and these structural changes are described. The absorption and resonance Raman spectral data for ^{Cu}cyt-*c* and model Cu–porphyrin complexes are shown to be consistent with electronic structure changes predicted by MO calculations and the four-orbital model of the excited electronic states of the porphyrin. Using an analysis in terms of the four-orbital model, we determine the changes in the frontier molecular orbitals necessary to account for the spectral shifts. The MO calculations for axial ligand complexes of Cu porphyrins are then shown to predict these shifts in orbital energies, and the calculations further suggest that the shifts result from addition of a σ-donating axial ligand. The relationship between changes in electronic structure and core expansion is discussed. Then, vibronic-coupling contributions to the β-band in ^{Cu}cyt-*c* are briefly examined. Finally, the influences of the vinyl groups in model Cu porphyrins and the thiol ether linkages in the protein are discussed.

Materials and Methods

The Cu(II) cytochrome *c* A form was prepared and purified by reported methods (Dickinson & Chien, 1975). The copper(II) derivatives of protoporphyrin IX (ProtoP), octaethylporphyrin (OEP), and uroporphyrin I (UroP) were obtained from Porphyrin Products and used without further purification. Pyridine (Fisher), piperidine (Aldrich), pyrrolidine (Aldrich), glass-distilled benzene and hexane (Burdick and Jackson), and 1-methylimidazole (Chemalog) were used as obtained. Samples were prepared by dissolving porphyrin powder in the appropriate solvent. UV–vis absorption spectra (Table I) agree with literature spectra except for Cu(ProtoP) in pyridine (Alston & Storm, 1979). Addition of a small

† From the Sandia National Laboratories, Albuquerque, New Mexico 87185 (J.A.S.), the VA Medical Center, Little Rock, Arkansas 72206 (K.D.S.), AT&T Bell Laboratories, Murray Hill, New Jersey 07974 (P.M.R.), and the University of Washington, Seattle, Washington 98195 (M.G. and E.R.D.). *Received November 9, 1983.* This work was performed at Sandia National Laboratories supported by the U.S. Department of Energy under Contract DE-AC04-76-DP00789 and the Gas Research Institute under Contract 5082-260-0767.

0006-2960/84/0423-3946$01.50/0

Table I: Peak Positions of UV–Vis Bands of Copper Porphyrins and Copper-Modified Heme Proteins

porphyrin	solvent	wavelength (nm)					type[a]
				B(0–0) (Soret)	Q(0–1) (β)	Q(0–0) (α)	
Cu(ProtoP)	10 mM Na_2HPO_4, 0.01% KCl[b]	249	315	398	532	570	M-4
	pyridine		340–350	409	537	573	M-4
				418–422	537–539	574–576	M-5
	pyridine, 1% 0.1 M NaOH		330–340	391	543	579	D-4
	pyridine[c]			387	538	575	D-4
	pyrrolidine			407	530–540	565–575	M-4
				424	545	579	M-5
	1-methylimidazole			407	534	571	M-4
				420–425	536–538	572–574	M-5
	0.05 M Mes buffer (pH 7.1), 0.05 M KCl[b]		335	385	540	577	D-4
	0.1 M NaOH/CTAB		335	406	532	571	M-4
Cu(ProtoP)DME	$CHCl_3$[c]			407			M-4
	piperidine[c]			413, 422			M-4
	piperidine at −15 °C			425			M-5
Cu(UroP)	0.1 M NaOH[d]		326	397	524	562	M-4
$[Cu(UroP)]_2$	0.1 M NaOH, 5.5 M NaCl		325	382	530	565	D-4
Cu(OEP)	$CHCl_3$, MeOH[e]			399	522	560	M-4
	benzene		326	398	525	562	M-4
	pyridine		328	398	526	562	M-4
	pyridine, 1% 0.1 M NaOH		326	398	525	561	M-4
	piperidine		348	398	530	566	M-4
				411	532–534	567–568	M-5
	pyrrolidine		351	398	533	563	M-4
				414	536–538	596–571	M-5
^{Cu}Mb	0.05 M Mes buffer (pH 7.1), 0.05 M KCl[c]	279	350	425	545	585	M-5
	10 mM phosphate buffer (pH 7.0), 0.01% KCl[b]	244	355–360	421	543		M-5
^{Cu}cyt-*c*	phosphate buffer (pH 6.5)	255	348	420	542	576	M-5
	phosphate buffer (pH 2.1)	262	325	389	532	567	D-4

[a] M-4, monomeric, 4-coordinate; M-5, monomeric, 5-coordinate; D-4, aggregated, 4-coordinate. [b] From Atassi (1967). Mes, 4-morpholineethanesulfonic acid. [c] From Alston & Storm (1979). [d] From Shelnutt (1983a). [e] From Smith (1975).

amount (1%) of aqueous sodium hydroxide to the neat pyridine solution causes shifts in the absorption maxima that are typical of π–π aggregation (see Table I), and upon centrifugation, precipitation of the porphyrin is observed. The absorption spectrum of the aggregate is close to the reported spectrum of Cu(ProtoP) in pyridine (Alston & Storm, 1979).

Raman spectra of ^{Cu}cyt-*c* were obtained simultaneously for either the neutral and acid forms or the neutral and alkaline forms with a Raman difference spectrometer previously described (Shelnutt, 1983a). Similarly, the Raman spectra of model Cu porphyrins and their complexes were obtained in pairs. The Raman spectra were obtained with either 514.5- or 528.7-nm excitation at about 300 mW from an argon ion laser (Coherent). The samples were irradiated in a partitioned cell rotating at 100 Hz. The spectral resolution is 2 cm^{-1}. From 6 to 15 scans were signal averaged and then smoothed by fast Fourier transform. On each scan of the region from 1280 to 1680 cm^{-1}, counts were accumulated for 0.5 s at each point of the spectrum for which the spectrometer (Spex) step size was 0.2 cm^{-1} for each data point. All Raman spectra were taken at room temperature (22 °C) unless noted.

Absorption spectra were recorded on a Perkin-Elmer Model 330 spectrophotometer. The pH of the ^{Cu}cyt-*c* samples was measured with a Fisher Acumet Model 750 pH meter.

Results

Figure 1 shows the absorption spectra of the neutral form (pH 6.5) and the low-pH form (pH 2.1) of the protein. The spectrum of the alkaline form of ^{Cu}cyt-*c* (not shown) is similar to that of the acid form. Note the large (31-nm) red shift of the Soret band of the neutral form. The α-band also shifts hypsochromically by 9 nm for the neutral pH form. The separation between the Q(0–0) (α-band) and B(0–0) (Soret band) decreases from 8070 cm^{-1} for the acid form to only 6450 cm^{-1} for the neutral form. In addition, either the N band near 325 nm gains considerable intensity and red shifts to 348 nm, or a new band at 348 nm has appeared. At pH 2.1 the spectrum is more typical of Cu(II) porphyrins in organic (Smith, 1975) or aqueous (Shelnutt, 1983a) solution.

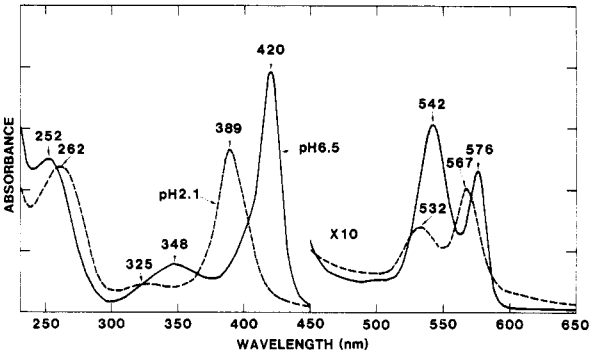

FIGURE 1: UV–vis absorption spectrum of copper cytochrome *c* at pH 6.5 (—) and at pH 2.1 (– –).

Figure 2 shows comparisons of Raman spectra of the marker band region for the neutral pH form of ^{Cu}cyt-*c* and the forms obtained at pH 2.1 and 13.0, respectively. At both pH extremes the Raman line frequencies are close to those observed for pyrrole-substituted Cu porphyrins (Shelnutt, 1983a; Spaulding et al., 1976). The region contains Raman lines sensitive to oxidation state (Spiro & Strekas, 1974; Spiro, 1982) and center-to-nitrogen distance (core size) (Spaulding et al., 1976; Spiro, 1982; Spiro et al., 1979). The frequencies of the Raman marker lines are shown in Table II.

Cu cytochrome *c* near neutral pH has a very unusual Raman spectrum for a copper porphyrin. The marker lines near 1500

Table II: Frequencies of Raman Marker Lines of Copper Porphyrins and Copper-Modified Heme Proteins

porphyrin	solvent	frequency (cm^{-1}) ν_4	ν_3	ν_{19}	ν_{10}	type[a]
Cu(ProtoP)	pyridine	1371			1635	M-4
	0.1 M NaOH/CTAB	1373	1500	1579	1636	M-4
	pyrrolidine[b]	1372			1629	M-5
Cu(ProtoP)DME	CS_2[c]	1373	1503	1584	1634	M-4
Cu(UroP)	0.1 M NaOH[d]	1379	1500	1582	1637	M-4
$[Cu(UroP)]_2$	0.1 M NaOH, 5.5 M NaCl[d]	1381	1503	1585	1640	D-4
Cu(OEP)	hexane	1378	1503	1582	1637	M-4
	CH_2Cl_2[e]	1381	1503	1584	1638	M-4
	benzene	1378	1504		1637	M-4
	piperidine[b]	1378	1503	1581	1632	M-5
	pyrrolidine[b]	1376		1580	1629	M-5
^{Cu}Mb	0.05 M Mes buffer (pH 7.1)	1374	1498	1580	1636	M-4
	0.05 M KCl[c]				1623	M-5
^{Cu}cyt-*c*	phosphate buffer (pH 6.5)	1372	1491	1570	1623	M-5
	phosphate buffer (pH 2.1)	1373	1500	1582	1637	D-4
	phosphate buffer (pH 13)	1373	1500	1581	1636	D-4

[a] Predominant species: M-4, monomeric, 4-coordinate; M-5, monomeric, 5-coordinate; D-4, aggregated, 4-coordinate. [b] The 5-coordinate species. Because complex formation is incomplete, the actual frequency may be lower than reported. [c] From Alston & Storm (1979). [d] From Shelnutt (1983a). [e] From Kitagawa et al. (1975).

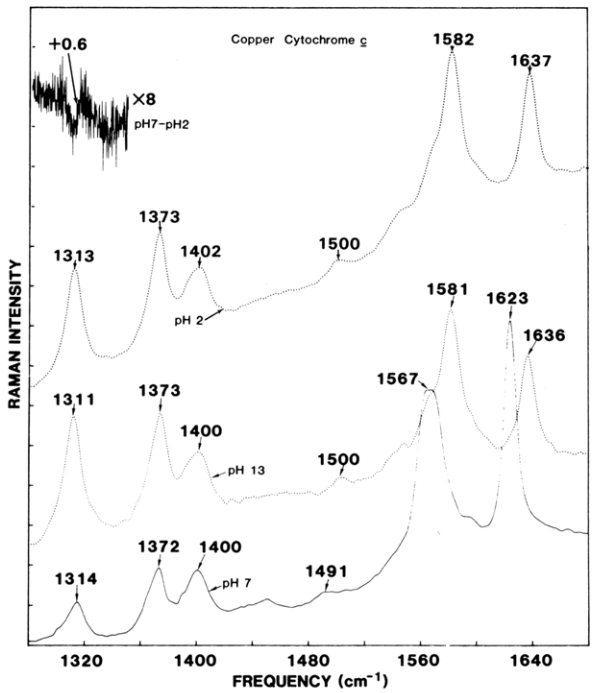

FIGURE 2: Resonance Raman spectra of copper cytochrome *c* at pH 6.5 (—), at pH 13 (···), and at pH 2.1 (···) and the Raman difference spectrum of the 1313-cm^{-1} Raman line. The difference spectrum is pH 7 − pH 2 (×8) and shows a deflection indicating a shift of −0.6 cm. Excitation is at 528.7 nm for the pH 2 Raman spectrum and at 514.5 nm for the pH 13 and 7 spectra.

(ν_3), 1582 (ν_{19}), and 1637 cm^{-1} (ν_{10}) for ^{Cu}cyt-*c* at either pH 2 or 13 are shifted from 9–15 cm^{-1} to lower frequency in the neutral form. These three Raman lines are well-known markers of the center-to-nitrogen (pyrrole) distance of metalloporphyrins (Spaulding et al., 1976; Spiro, 1982; Spiro et al., 1979).

On the other hand, the Raman line at 1373 cm^{-1} (ν_4) is the oxidation-state and π-charge-density marker line of iron porphyrins and heme proteins (Shelnutt, 1983a–c; Spiro & Strekas, 1974; Spiro, 1982). The frequency of ν_4 for ^{Cu}cyt-*c* is about 1 cm^{-1} lower at neutral pH than at the pH extremes. The frequency of ν_4 is also about 6 cm^{-1} lower than that for water-soluble model Cu porphyrins (Shelnutt, 1983a, 1981) and Cu octaethylporphyrin in noncoordinating solvents (Spaulding et al., 1976). The 1313-cm^{-1} (ν_{21}) vibration, which

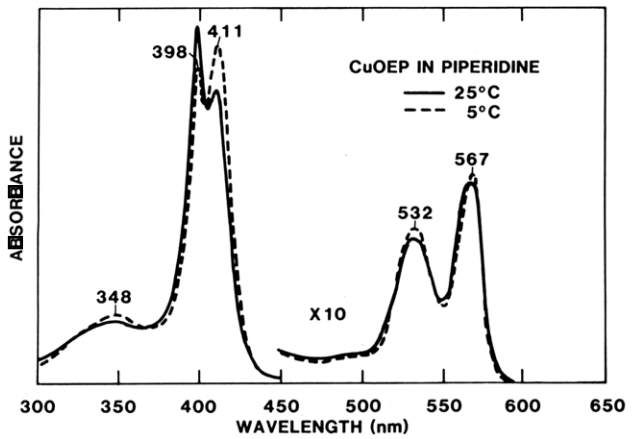

FIGURE 3: Absorption spectrum of copper octaethylporphyrin in piperidine at 25 (—) and 5 °C (--).

is sensitive to substituent orientation (Adar, 1975, 1977; Shelnutt et al., 1979a, 1981a) and aggregation (Shelnutt, 1981; Shelnutt et al., 1984), as well as ring π-charge density (Shelnutt, 1983a; Spiro, 1982; Spiro & Burke, 1976), shifts 0.6 cm^{-1} lower at low pH but shifts by almost 3 cm^{-1} lower relative to the neutral form at high pH.

The absorption spectra of Cu(OEP) in piperidine at 25 and at 5 °C are shown in Figure 3. Two Soret bands are noted with maxima at 398 and 411 nm. On a lowering of the temperature, the red-shifted Soret band gains intensity at the expense of the blue Soret, indicating increasing coordination with piperidine. The Soret at 398 nm is typical of Cu(OEP) in noncoordinating solvents such as benzene (Table I) or *n*-hexane. Also associated with increased complexation at low temperature are a slight decrease in α/β ratio and a small red shift of the visible bands. In addition, the UV band at 348 nm increases in intensity.

Figure 4 shows a comparison of the resonance Raman spectra of 4-coordinate Cu(OEP) in hexane and the piperidine–Cu(OEP) complex. In spite of only partial formation of a 5-coordinate complex, it is clear that the core-size marker lines are shifted to lower frequency by up to 5 cm^{-1}. The spectra of the pyrrolidine–Cu(OEP) complex and 4-coordinate Cu(OEP) in hexane at −20 ± 10 °C shown in Figure 4 were obtained simultaneously on the Raman difference spectrometer and, therefore, can be accurately compared. At low temperature the 5-coordinate pyrrolidine complex dominates, and

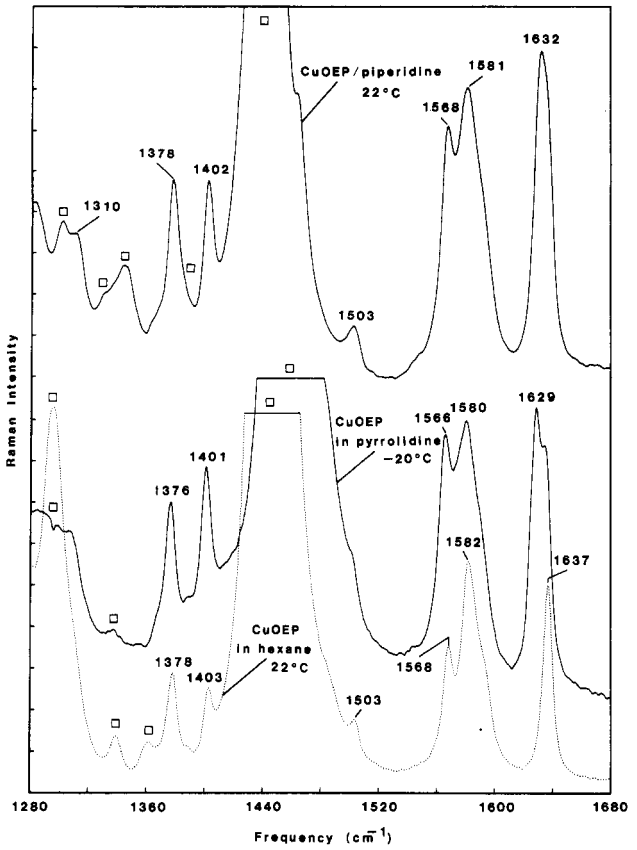

FIGURE 4: Resonance Raman spectra of copper octaethylporphyrin in piperidine (—) at 22 °C and in pyrrolidine (—) and hexane (···) at −20 °C. Cu(OEP) in pyrrolidine and in piperidine is a mixture of 4- and 5-coordinate forms. Boxes indicate solvent lines.

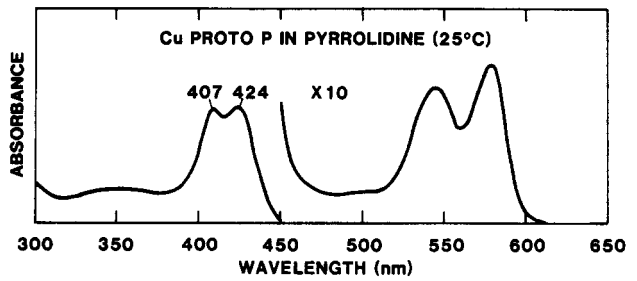

FIGURE 5: Absorption spectrum of copper protoporphyrin IX in pyrrolidine at 25 °C.

2–8-cm^{-1} decreases in frequencies of the core-size marker lines relative to 4-coordinate Cu(OEP) are observed.

The shifts in ν_4 are smaller than those for the core-size marker lines. The 5-coordination results in only a ~2-cm^{-1} decrease for the pyrrolidine complex, and the Raman difference spectra give ν_4 only 0.4 cm^{-1} lower relative to Cu(OEP) in benzene for the piperidine–Cu(OEP) complex. Thus, although the complex-induced shifts are smaller, they show the same pattern as noted for the ^{Cu}cyt-*c* neutral form, i.e., smaller shifts in ν_4 than in the core-size marker lines.

Cu(ProtoP) forms similar coordination complexes in strong bases as shown in Figures 5 and 6. The Soret band, α-band, and β-band of the protoporphyrin derivative (Figure 5) are red shifted by the vinyls at the 2 and 4 positions relative to the OEP spectrum. Furthermore, the Soret of the pyrrolidine complex is again strongly red shifted (17 nm) relative to the Soret of the 4-coordinate form. At 25 °C, the complex exists in about equal proportions with the 4-coordinate form; at 5 °C, the Soret of the complex gains intensity, the α-band shifts slightly to the red, and the α/β ratio decreases about 3%.

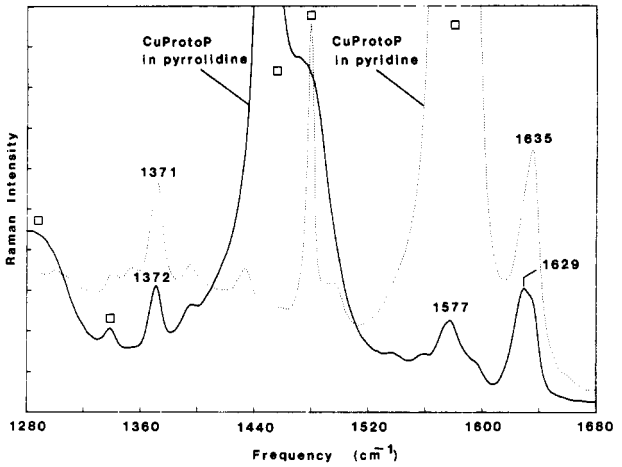

FIGURE 6: Resonance Raman spectra of copper protoporphyrin IX in pyrrolidine (—) and in pyridine (···) at 22 °C. Cu(ProtoP) in pyrrolidine is a mixture of 4- and 5-coordinate forms as indicated by the shoulder on the ν_{10} line at 1629 cm^{-1}. Boxes indicate solvent lines.

The Raman spectrum of the mixture of 4-coordinate Cu(ProtoP) and pyrrolidine–Cu(ProtoP) complex is compared with the predominately 4-coordinate Cu(ProtoP) in pyridine in Figure 6. The mixture of 4- and 5-coordinate forms shows shifts of the marker lines to low frequency for the pyrrolidine–Cu(ProtoP) complex. As for the other Cu–porphyrin 5-coordinate complexes, the shifts are most evident for the vibration at 1629 cm^{-1}. A shoulder at the 4-coordinate frequency (1635 cm^{-1}) clearly indicates the presence of a 4-coordinate component. The oxidation state line ν_4 at 1372 cm^{-1} in the 4-coordinate form is lower by 0.6 ± 0.2 cm^{-1} in the 5-coordinate complex.

Table I gives the positions of the absorption band maxima for copper-modified proteins and relevant model compounds. The Soret bands of monomeric, 4-coordinate copper porphyrins are in the range 397–413 nm. Examples are Cu(OEP) in $CHCl_3$/MeOH and Cu(UroP) in 0.1 M NaOH. The 5-coordinate, monomeric Cu porphyrins give red-shifted Soret bands between 411 and 425 nm. Known dimeric model porphyrins, such as Cu(UroP) in aqueous 5.5 M salt solution, have blue-shifted Soret bands near 382–391 nm. The Soret band of the acidic form (pH 2) of ^{Cu}cyt-*c* at 389 nm is consistent with porphyrin π–π dimerization. ^{Cu}cyt-*c* is known to dimerize such that the porphyrin moieties are also dimerized with a Cu–Cu distance of 4.2 Å—a distance compatible with π–π aggregation (Blumberg & Peisach, 1965; Chikira et al., 1980). From this classification of spectra, it is apparent that approximately half of the large pH-dependent red shifit (31 nm) of the Soret band of ^{Cu}cyt-*c* results from breaking up the dimer, and the rest is caused by formation of the 5-coordinate complex. Further, the increase in width of the absorption bands for the pH 2.1 form (Figure 1) results from dimerization. A similar broadening and rising background absorbance in the Q-band region are observed for Cu(UroP) dimer (Blumberg & Peisach, 1965; Shelnutt, 1983a; Shelnutt et al., 1984).

Dimerization of either Cu(UroP) (Shelnutt, 1983a; Shelnutt et al., 1984) or urohemin (Shelnutt, 1983c; Shelnutt et al., 1984) results in shifts in the Raman marker lines to higher frequency relative to the monomer values. The shifts in ν_4 and the core-size lines are of about equal magnitude (2–3 cm^{-1}), in contrast with ligation-induced shifts noted above (Shelnutt, 1983a; Shelnutt et al., 1984). Attempts to compare the neutral pH form of ^{Cu}cyt-*c* and forms that exist at pH extremes are hindered by the fact that both axial ligation and aggregation

occur. Therefore, it is not certain that the smaller aggregation-induced Raman shifts are present. The aggregation of Cu(ProtoP) in pyridine with added aqueous base (Table I) apparently results from deprotonation of the propionic acid groups, since addition of base to Cu(OEP) in neat pyridine does not produce shifts characteristic of π–π aggregation.

Discussion

Background. Recent studies of ^{Cu}cyt-*c* (Findlay et al., 1977; Chikira et al., 1980; Straub & Rentzepis, 1983) have focused mainly on electron paramagnetic resonance (EPR), absorption spectroscopy, and emission relaxation studies. Nuclear magnetic resonance (NMR) of paramagnetic ^{Cu}cyt-*c* gives poor-quality spectra (Moore et al., 1980) and, thus, has not been used extensively. However, NMR studies of Fe(II), Co(III), and Zn(II) cytochromes *c* have shown the conformation of these proteins to be only slightly modified in the region of the chromophore by metal substitution (Moore et al., 1980). In particular, the axial ligands of the cobalt and zinc derivatives were found to be the same as in native cytochrome *c*, i.e., histidine-18 and methionine-80.

EPR studies have been most useful in determining the state of coordination of the Cu(II) ion. Findlay et al. (1977) found that ^{Cu}cyt-*c* forms dimers below pH 4 and above pH 11. They also interpreted absorption and EPR spectra of the neutral pH form as indicating a monomeric, 6-coordinate Cu ion. They determined the ordering of the d orbitals as $d_\pi < d_{xy} < d_{z^2} < d_{x^2-y^2}$ with $d_{x^2-y^2}$ being the singly occupied orbital. Chikira et al. (1980) later observed the $\Delta M = 2$ transitions, thereby demonstrating that the Cu porphyrins themselves dimerize at the pH extremes with the Cu–Cu distance of about 4.2 Å. They further identified two types of monomers that exist above and below pH 6. Because of the similarity of the EPR parameters of the low-pH monomer to monomeric Cu porphyrins in noncoordinating solvents, the pH 4–6 monomer is thought to be 4-coordinate. The neutral pH monomeric form is 5-coordinate on the basis of similarity of the EPR parameters to those of the reported pyrrolidine monoadduct of Cu(II) octaethylporphyrin (Chikira et al., 1979; Baker et al., 1964) and Cu(II) myoglobin (^{Cu}Mb), in which Cu is bound only to the imidazole of proximal histidine (Alston & Storm, 1979).

Myoglobin reconstituted with Cu(II) protoporphyrin IX has been examined by UV–vis absorption spectroscopy, EPR, circular dichroism, quantitative analysis, immunochemistry, and resonance Raman methods (Alston & Storm, 1979; Atassi, 1967; Andres & Atassi, 1970). These results show that ^{Cu}Mb contains one specifically bound Cu(ProtoP) per globin molecule (Atassi, 1967) and that the protein conformation is very similar to native metMb (Atassi, 1967; Andres & Atassi, 1970). EPR spectroscopy strongly supports a 5-coordinate Cu in ^{Cu}Mb at pH 7 on the basis of the similarity of its EPR parameters to 5-coordinate Cu–porphyrin axial complexes with bases such as piperidine (Alston & Storm, 1979; Atassi, 1967).

The red shift in the Soret band by about 10 nm relative to copper porphyrins in noncoordinating solvents also supports a 5-coordinate complex in ^{Cu}Mb (Chikira et al., 1979; Baker et al., 1964; Alston & Storm, 1979). The α/β-band absorbance ratio (about 1) is also greatly reduced in ^{Cu}Mb relative to 4-coordinate copper porphyrins (about 1.4), although the ratio is not inverted as is the case for ^{Cu}cyt-*c*. The α- and β-bands are also red shifted by several nanometers as is observed for ^{Cu}cyt-*c* (see Table I). The red shifts and decrease in α/β ratio were explained (Alston & Storm, 1979) in terms of increased charge density in the porphyrin ring resulting from axial coordination in analogy with the effects of varying electronegativity in a series of metalloporphyrins (Gouterman, 1959; Shelnutt, 1983b; Shelnutt & Ondrias, 1984).

Resonance Raman spectra of ^{Cu}Mb in the high-frequency marker line region are similar to the model 4-coordinate Cu(ProtoP) dimethyl ester (DME) (Alston & Storm, 1979). The oxidation-state marker line (ν_4) occurs at 1374 cm^{-1} in ^{Cu}Mb and at 1373 cm^{-1} in Cu(ProtoP)DME. However, the frequency of ν_3 is 5 cm^{-1} lower in ^{Cu}Mb (1498 cm^{-1}) than for Cu(ProtoP)DME. The other core-size marker lines between 1550 and 1650 cm^{-1} could not be identified in the complicated Raman spectrum of ^{Cu}Mb obtained with 457.9-nm excitation (Alston & Storm, 1979).

Core Expansion in Copper Cytochrome c. In contrast with ^{Cu}Mb and the model complexes, the changes in the absorption spectrum and Raman marker line frequencies are more dramatic in the case of copper cytochrome *c* at pH 7. For example, the α/β intensity ratio is reduced to a greater extent compared to ^{Cu}Mb, and the core-size marker lines (ν_3, ν_{19}, and ν_{10}) exhibit larger decreases in frequency (Table II). These larger spectral changes indicate a similar but enhanced effect of axial ligation for the neutral form of ^{Cu}cyt-*c* relative to ^{Cu}Mb.

The ν_3, ν_{19}, and ν_{10} vibrations are sensitive to oxidation state, as well as to core size. However, since the frequency of the oxidation state marker line ν_4 changes by only 1 cm^{-1} at the pH extremes, the major effect on ν_3, ν_{19}, and ν_{10} results from an increase in center-to-nitrogen distance in the neutral pH form. We can calculate the expansion of the porphyrin core that accompanies axial ligation in the neutral pH form of ^{Cu}cyt-*c* from the correlations given by Spiro (1982). The shifts in the core-size marker lines indicate an expansion of the porphyrin core by about 0.03 Å for the neutral form of ^{Cu}cyt-*c*. The exact change in core size found depends on whether the shift in ν_3, ν_{19}, or ν_{10} is used in the calculation, but the range is from 0.02 to 0.03 Å.

The expansion of the core for the neutral pH form of copper cytochrome *c* cannot result from in-plane movement of the metal atom because the metal atom is already in plane for the extreme pH forms. This conclusion is reached because the Raman frequencies and absorption spectrum of the acid and alkaline forms are typical of Cu porphyrins in aqueous and organic, noncoordinating solvents (Table I), which are known to contain in-plane Cu(II). Most likely, the ring vibrations are influenced by a change in the interaction of the copper ion with the porphyrin ring resulting from pH-dependent changes in axial ligation. Such large shifts in the core-size marker lines represent relatively large changes in the metal–porphyrin interaction, since the shifts are roughly the same magnitude as shifts in these lines accompanying spin-state changes in Fe porphyrins (Spiro & Burke, 1976).

Origin of Shifts in the $\pi \rightarrow \pi^*$ Absorption Bands of Copper Cytochrome c. A detailed analysis of the changes in the electronic structure of the porphyrin ring using the four-orbital model (Gouterman, 1959) can give insight into the nature of the unusual axial ligation that occurs in ^{Cu}cyt-*c* at neutral pH. In this model the α-band and Soret band arise from electronic transitions originating from the top-filled molecular orbitals, $a_{1u}(\pi)$ and $a_{2u}(\pi)$, to the lowest empty $e_g(\pi^*)$ orbital. Because of near degeneracy of the $a_{1u}(\pi)$ and $a_{2u}(\pi)$ orbitals and because the excited-state electronic configurations have the same symmetry (E_u), the excited-state configurations strongly interact via the electron–electron repulsion term of the molecular Hamiltonian. Transitions to the configuration-interaction mixed excited states, called Q and B, give the α-band and Soret band, respectively. The β-band is the vibrationally induced Q(0–1) band (Perrin et al., 1969). Differences in the $\pi \rightarrow$

π^* bands that result from varying the metal in the porphyrin core can be treated in the four-orbital model as a totally symmetric perturbation on these electronic states (Gouterman, 1959).

Axial ligation sometimes causes spectral changes that are similar to changes observed with different metals and can be treated similarly as a perturbation. Axial ligand changes in vanadium(IV) porphyrins are one example. The change from an oxo to a dihydroxy complex of vanadium uroporphyrin results in shifts in α-band and Raman marker lines that maintain the same relationship between these spectral parameters as is noted for metal substitution (Kitagawa et al., 1975; Shelnutt & Ondrias, 1984; Shelnutt & Dobry, 1983).

The changes in the Raman and absorption spectrum of ^{Cu}cyt-*c* are also of this type; therefore, we assume that axial ligation at neutral pH merely modifies the metal–porphyrin interaction and can be treated within the four-orbital model. Three parameters given by Gouterman (1959) characterize the absorption spectrum:

$$E_{BQ} = E_B - E_Q = 2A_{1g}''(1 + \theta^2) \quad (1)$$

$$E_Q = A_{1g}' - A_{1g}''(1 + \theta^2) \quad (2)$$

$$f_Q \sim \theta^2 E_Q f_B / E_B \quad (3)$$

where $2\theta = A_{1g}/A_{1g}'' \ll 1$ is a parameter that "unmixes" the electronic states obtained from equal mixtures of the singly excited electronic configurations. E_Q is the energy of the α-band, E_{BQ} is the separation of the α-band and Soret band; f_Q is the integrated intensity of the α-band. A_{1g}'' is the two-electron exchange integral mixing the excited-state configurations and is considered a constant close to 3350 cm^{-1} (Gouterman, 1959). In the four-orbital model, A_{1g} is the separation of the $a_{1u}(\pi)$ and $a_{2u}(\pi)$ orbital energies, and A_{1g}' is the average of the energies for the transitions from the a_{1u} and a_{2u} orbitals to $e_g(\pi^*)$. A_{1g} and A_{1g}' are assumed to change, thereby producing the spectral changes observed for the neutral form of ^{Cu}cyt-*c*.

In terms of the parameters E_{BQ}, E_Q, and f_Q the changes observed for the neutral form relative to the alkaline or acid forms are (1) the frequency of the Q-band maximum E_Q decreases by 280 cm^{-1}, (2) the separation of the Q and B bands E_{BQ} decreases by 1620 cm^{-1}, and (3) f_Q, the oscillator strength of the Q band, decreases. [Depending upon how much of the rising background absorbance of the low-pH form (Figure 1) is subtracted, the ratio of the integrated intensities of the α-bands is between 0.71 and 0.96.]

When the changes in E_Q, f_Q, and E_B are considered, the decrease in oscillator strength f_Q is consistent with a decrease in θ^2 for the neutral form of ^{Cu}cyt-*c* relative to the extreme pH forms. A decrease in θ^2 also lowers the separation of Q and B (eq 1). However, a decrease in θ^2 by itself increases E_Q; therefore, A_{1g}' must decrease more than $A_{1g}''(1 + 2\theta^2)$ to account for the red shift in the band. Hence, changes in the spectrum at pH 7 can be explained in terms of a modified metal–porphyrin interaction that induces a decrease in both A_{1g}' and $|A_{1g}|$ (i.e., θ^2) relative to their values at acid or alkaline pH.

In the four-orbital model, the changes in A_{1g} and A_{1g}' are given by [eq 8 in Gouterman (1959)]

$$\Delta A_{1g} = (1/2)(\delta a_1 - \delta a_2) \quad (4)$$

$$\Delta A_{1g}' = (1/2)(2\delta e - \delta a_1 - \delta a_2) \quad (5)$$

where δe, δa_1, and δa_2 are the changes in the energies of the $e_g(\pi^*)$, $a_{1u}(\pi)$, and $a_{2u}(\pi)$ orbitals, respectively. The $a_{1u}(\pi)$ orbitals has nodes at the pyrrole nitrogens, and hence, it does not interact directly with the metal atom. Here, we are using the fact that axial ligation in ^{Cu}cyt-*c* influences the porphyrin only through the "usual" metal–porphyrin interaction. Therefore, δa_1 vanishes approximately for the metal–porphyrin interaction, and

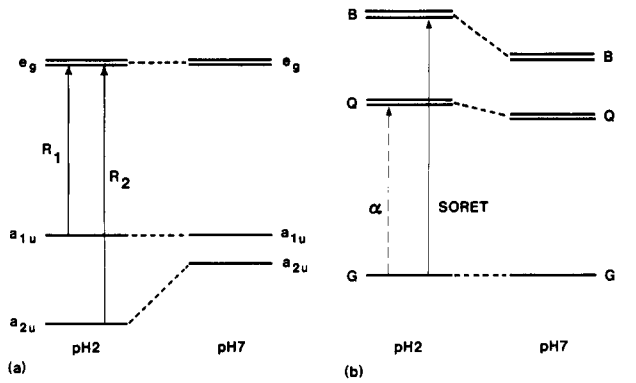

FIGURE 7: Schematic of changes in orbital energies (a) and state energies (b) capable of producing observed shifts in the absorption and Raman spectra of the neutral form of copper cytochrome *c* and 5-coordinate copper–porphyrin complexes.

$$\Delta A_{1g} = -(1/2)\delta a_2 \quad (6)$$

$$\Delta A_{1g}' = \delta e - (1/2)\delta a_2 \quad (7)$$

The change in $A_{1g} = E(a_{1u}) - E(a_{2u})$ is positive or negative depending on whether the a_{2u} or a_{1u} orbital is higher in energy. Molecular orbital calculations predict the near degeneracy of the a_{1u} and a_{2u} orbitals, but differ, depending on the calculational method, as to which of the two orbitals is higher. IEH MO calculations for Cu–porphine (P) put the a_{2u} orbital higher, but other methods, including some ab initio MO calculations, find the a_{1u} orbital in metalloporphyrins is higher than a_{2u} (Kashiwagi & Obara, 1981; Petke et al., 1978; Roos & Sundbom, 1970). However, Spellane et al. (1980) have shown that the spectra of a series of metalloporphyrins are explained if the a_{1u} orbital is actually the higher of the two for β-carbon-substituted metalloporphyrins. We would, nevertheless, expect the IEH calculations to predict the changes in orbital energies, even though the absolute ordering of these nearly degenerate orbitals is incorrectly predicted. Because a_{1u} is above a_{2u}, an increase ($\delta a_2 > 0$) in a_{2u} energy will decrease $|A_{1g}|$. Since $\theta^2 \sim A_{1g}^2$ must decrease to account for the decrease in E_{BQ}, we see that the a_{2u} level must be raised by the interaction of the metal atom with its axial ligand(s). As mentioned earlier, A_{1g}' must also decrease in order to account for the red shift in the Q band. Note that the increase in a_{2u} energy is sufficient to ensure that $\Delta A_{1g}'$ will also be negative as long as δe is small or negative.

The case where $\delta e = 0$ is illustrated in Figure 7. A shift only in the $a_{2u}(\pi)$ energy is seen to be sufficient to qualitatively account for the shifts in the Soret band and α-band. In particular, a larger red shift is predicted for the Soret band than for the α-band, as is observed.

This simple model also qualitatively predicts the changes in band intensities. The model predicts a decrease in oscillator strength of the α-band for the pH 7 form. A decrease in integrated intensities appears to be observed. However, a strong background absorbance from the tail of the Soret in the α-band region of the high- and low-pH forms makes quantification of the decrease difficult (−15 ± 10%). The background absorbance is a result of broadening of the bands caused by dimerization. Similar absorption and resonance Raman spectral changes are observed (Shelnutt & Dobry, 1983) upon change of axial ligands in vanadium(IV) uro-

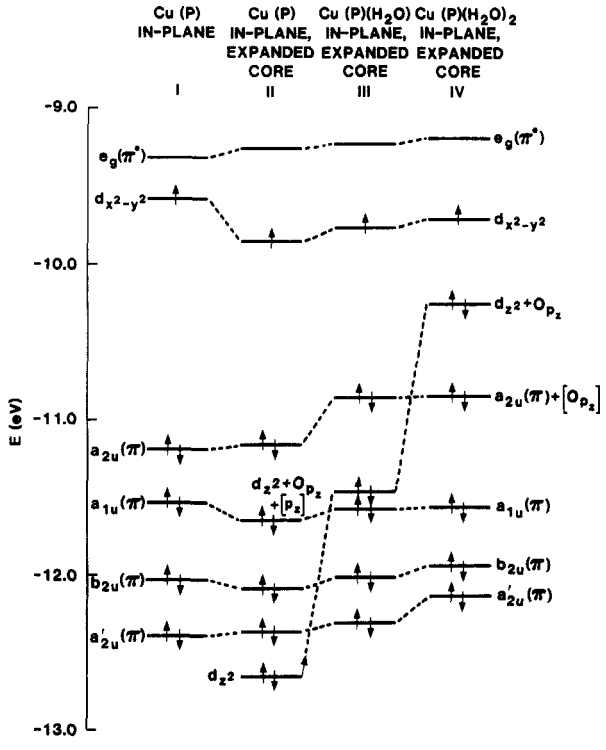

FIGURE 8: Orbital energies from IEH molecular orbital calculations for indicated geometries and axial ligands. IEH MO calculations invert the ordering of the a_{1u} and a_{2u} orbitals.

porphyrin from V=O to $V(OH)_2$. In this case, however, the broadening does not occur, and the Q-band oscillator strength decreases considerably (30%) as predicted.

Molecular Orbital Calculations: Copper Cytochrome c Electronic Structure. These conclusions are further supported by IEH molecular orbital calculations. Moreover, an explanation of the strong band at 348 nm is suggested by the MO picture. Figure 8 shows results of perturbations of the in-plane Cu porphyrin structure and the effect of metal coordination by a basic ligand, modeled by water. (Remember that the IEH calculations invert the ordering of the a_{1u} and a_{2u} orbitals.)

Expansion of the porphyrin core by 0.07 Å (twice the observed expansion) alone has a significant effect on $E(a_{1u}) - E(a_{2u})$ as the a_{1u} and a_{2u} levels shift in opposite directions. However, addition of an axial ligand has a much larger effect. The a_{2u} level increases by 0.25 eV (2000 cm^{-1}), while the a_{1u} orbital remains relatively constant. Also, the d_{z^2} metal orbital is raised to the level of the frontier orbitals as a result of mixing with the filled p_z orbital of the water oxygen atom. The metal d_{z^2} orbital becomes mixed with porphyrin orbitals, primarily a_{2u}, as well. Calculations (not illustrated in Figure 8) show that an out-of-plane position of the Cu ion has little effect on the energies. However, addition of a second water molecule further raises the energy of d_{z^2}, but because of the higher effective symmetry, it is not significantly mixed with the porphyrin orbitals. A large change in the splitting of the $a_{2u}'(\pi)$–$b_{2u}(\pi)$ orbital pair, which give rise via CI interaction to the N and L bands in the UV spectrum, does occur.

Axial ligation to Cu is seen to give a large increase in the a_{2u} energy consistent with the changes in the optical spectrum as described above (Figure 7). The strong band at 348 nm (pH 7) appears to result from a metal d_{z^2} to porphyrin $e_g(\pi^*)$ charge-transfer transition, possibly gaining intensity from mixing of d_{z^2} with porphyrin orbitals. An explanation based on the appearance of a new charge-transfer band is preferred because a shoulder at the position of the N band at 325 nm is still evident in the pH 7 ^{Cu}cyt-*c* spectrum. Selective enhancement of axial ligand and metal–nitrogen (pyrrole) modes is a possibility (Shelnutt et al., 1976) for laser excitation in the new band at 348 nm. Other ligand → metal and metal → ligand charge-transfer transitions, i.e., those involving the $d_{x^2-y^2}$ orbital, are shifted in energy. Kim et al. (1984) have explained the fast relaxation of 5-coordinate Cu porphyrins by a red shift of the $a_{2u}(\pi) \rightarrow d_{x^2-y^2}$ transition with coordination as shown in Figure 8.

Others (Gouterman et al., 1973; Nappa & Valentine, 1978; Alston & Storm, 1979) have attributed the red shifts in the absorption spectrum to an increase in charge on the porphyrin ring. Indeed, the MO calculations show an increase in ring charge of 0.14 electron when an H_2O ligand is added (III in Figure 8).

Relationship between Core Expansion and Porphyrin Electronic Structure. The Raman data also support a pH-dependent change in the $a_{2u}(\pi)$ orbital's interaction with the metal. Metal-dependent stabilization of the $a_{2u}(\pi)$ orbital and the associated α-band shift are correlated with increased core-size marker line frequencies (Kitagawa et al., 1975; Shelnutt, 1983b; Shelnutt & Ondrias, 1984). Further, the relative magnitudes of shifts in core-size and oxidation-state marker lines that are observed upon metal substitution (Shelnutt, 1983b; Shelnutt & Ondrias, 1984) are similar to the pH-dependent shifts observed in ^{Cu}cyt-*c* and in the 5-coordinate Cu–porphyrin complexes. That is, the shift for ν_4 is much smaller than those for ν_3, ν_{19}, and ν_{10}. The core-size marker lines primarily involve C_α–C_m stretching (Abe et al., 1978) and are expected to be influenced by π-charge at the meso carbons. The a_{2u} orbital has large coefficients on C_m; thus, it is reasonable that a change in a_{2u} conjugation with the metal should be associated with core-size marker line shifts. [This pattern of shifts was also observed for π–π charge-transfer complexes with aromatic acceptors (Shelnutt, 1983b,c). The top-filled a_{1u} and a_{2u} orbitals are likely donor orbitals in these complexes. Here again, changes in the a_{2u} level are associated with shifts in the core-size marker lines.]

Axial Ligation in Copper Cytochrome c at Neutral pH. On the basis of the above discussion of effects of changes in the metal's interaction with the ring, inferences about how axial ligation induces these changes can be made. Copper(II) is d^9 and has no empty 3d orbitals available to receive π-donation from an axial ligand. On the other hand, σ-donation to the unoccupied $4p_z$ orbital of the metal is possible. Charge donation to the $4p_z$ orbital raises its energy. The increased separation between the metal p_z orbital and the porphyrin $a_{2u}(\pi)$ orbital decreases their interaction, destabilizing $a_{2u}(\pi)$. The MO calculations support this interpretation. As discussed above, destabilization of a_{2u} results in lower frequencies for the core-size marker lines and in a red shift of the Q and B absorption bands in the neutral form of ^{Cu}cyt-*c* when the configuration interaction is considered. Thus, strong σ-bonding alone qualitatively accounts for the spectral changes.

The protein matrix about the copper–porphyrin appears to exert considerable influence over axial ligation, especially in ^{Cu}cyt-*c*. This statement is based on several discrepancies between the spectra of ^{Cu}cyt-*c* and ^{Cu}Mb and the model compounds. First, inversion of the α/β intensity ratio is observed only for the proteins. Also, strong red shifts in the α- and β-bands are not observed for the model Cu porphyrins. Finally, the Raman core-size marker lines shift to a greater extent in ^{Cu}cyt-*c* than in the models. Nevertheless, similarities in the spectral changes, including the appearance of a new UV band, suggest that the difference lies in the degree of ligand interaction, not in the mechanism. It may simply be that complex

formation is complete in the protein and that the field strength of the ligand "forced onto" the copper ion by the protein is higher than any ligand that forms a solution complex.

Intensity of the β-Band: Vibronic Coupling. Another major change in the absorption spectrum is the large increase in the β-band for the pH 7 form. The intensity resulting from vibronic coupling of Q and B states contributed by the Lth normal mode is proportional to (Shelnutt, 1981b)

$$\frac{f_B(h^L_{BQ})^2}{E_B} \frac{\cos^2\theta}{(E_B - E_Q - \hbar\omega_L)^2}$$

where $E_B - E_Q = 2A_{1g}''(1 + \theta^2)$ and h^L_{BQ} is the electronic part of the vibronic coupling matrix element for the mode of frequency $\hbar\omega_L$. All but the last factor are nearly constant so the ratio of vibronic intensity for the neutral to acid pH forms is approximately $[(8070 - 1500)/(6450 - 1500)]^2 = 1.8$. This value is in fair agreement with the experimental integrated intensity ratio that is between 1.9 and 2.2, depending on how the background absorption for the pH 2 form is treated. Vibronic coupling within the Q-state vibrational manifold via Jahn–Teller active and Franck–Condon active (totally symmetric) normal modes also contributes to β-band absorbance (Shelnutt, 1981b).

Additional Comparisons with Model Copper Porphyrins. Several other useful conclusions result from further consideration of the model Cu porphyrin absorption and Raman spectra. Monomeric, 4-coordinate Cu porphyrins without vinyl substituents have α-bands from 560 to 564 nm, and Soret bands are in the range 397–399 nm; monomeric, 4-coordinate Cu(ProtoP) in various solvents has α-bands from 570 to 573 nm, and Soret bands are near 407 nm. Thus, substitution of two vinyl groups for alkyl groups results in a red shift of about 10 nm in both the α-band and Soret band (Adar, 1975; Falk, 1964). Because a_{2u} places little charge on the β-carbons, the best bet is that $\delta a_2 \approx 0$. On the other hand, the $e_g(\pi^*)$ orbital places considerable charge on the β-carbons, and conjugation of the vinyls with the ring π-system might be expected to stabilize $e_g(\pi^*)$.

This interpretation of the effects of vinyl conjugation on porphyrin orbitals is also consistent with the Raman shifts. The Raman marker lines are not influenced by kinematic substituent effects upon vinyl deuteration (Choi et al., 1982) but may be influenced electronically by the vinyls. Since ν_{10} is sensitive to the a_{2u} orbital level and $\delta a_2 \approx 0$, we predict ν_{10} will be relatively insensitive to vinyl conjugation. Comparison of ν_{10} for Cu(ProtoP) with Cu(OEP) and Cu(UroP) (monomeric, 4-coordinate species) shows a less than 3-cm^{-1} decrease in ν_{10}.

The oxidation state marker line ν_4, however, is sensitive to $e_g(\pi^*)$, which can be influenced by the vinyls. The frequency of ν_4 is from 3 to 8 cm^{-1} lower for Cu(ProtoP) than for Cu(OEP) or Cu(UroP), consistent with a relatively large vinyl influence on $e_g(\pi^*)$. However, it should be noted that ^{Cu}cyt-*c*, which has saturated vinyls, also exhibits low frequency for ν_4.

In cytochrome *c* peroxidase, ν_4 changes frequency with pH, and the pK for the transition is the same as that of a group of the protein that controls its catalytic and ligand binding activity (Shelnutt et al., 1983). Further, of the identified proton resonances of the heme, only the α-proton of the 4-vinyl group shifts with pH, and its pK is also the same as the controlling group of the protein (Satterlee et al., 1983). The shift in the vinyl proton resonance is associated with the planarity of the vinyl with the porphyrin ring. Thus, as the 4-vinyl group moves into a more planar orientation and, hence, becomes more conjugated with the ring, the frequency of ν_4 increases. This relationship between ν_4 and planarity of the vinyl is consistent with the above interpretation of the effects of vinyl conjugation on the absorption bands and Raman lines.

Conclusions

Gross changes in the absorption and resonance Raman spectra of ^{Cu}cyt-*c* occur upon varying the pH. At pH 2 and 13 the spectra are typical of Cu(II) porphyrin dimers in solution. However, near neutral pH, unusual copper porphyrin spectra are observed. The spectra are consistent with 5-coordinate Cu porphyrins; no evidence for 6-coordination is found. Previously, Findlay et al. (1977) and Reynolds et al. (1982) suggested 6-coordination to account for the larger shift in the Soret band (31 nm) than is usually associated with 5-coordination. However it is now clear that 15–18 nm of the shift is the result of π–π dimerization of the Cu porphyrin moieties at the pH extremes.

The Raman marker-line shifts indicate expansion of the porphinato core by 0.03 Å in the neutral form, and a smaller expansion of the core occurs upon formation of the 5-coordinate species for the model Cu porphyrins. Since π–π dimerization results in only small marker-line shifts, the expanded core is a result of axial ligation and its effect on the porphyrin–metal interaction.

A detailed analysis of the changes in the absorption spectrum due to axial ligation shows them to be consistent with decreased metal conjugation with the porphyrin ring in the anomalous neutral pH form of the protein. The spectral changes are similar to the result of substitution of a less electronegative metal than Cu, e.g., Mg. Strong σ-bonding of the axial ligand is imposed by the protein moiety at neutral pH. A weak π-bonding or inductive effect of the axial ligand cannot be ruled out. The part of the red shifts of the $\pi \rightarrow \pi^*$ absorption bands that is induced by addition of the fifth ligand is explained by destabilization of the a_{2u} orbital. Raman marker-line shifts also are consistent with destabilization of the $a_{2u}(\pi)$ orbital. MO calculations predict that the new UV band near 350 nm in the 5-coordinate complexes and copper proteins at neutral pH results from a $d_{z^2} \rightarrow \pi^*$ charge-transfer transition.

Copper cytochrome *c* and model copper–porphyrins provide a unique porphyrin system in which a simple electronic structure change, i.e., σ-donation to metal resulting from axial ligation, is well characterized in terms of its effect on the frontier molecular orbitals of the ring. Changes in the π-orbitals qualitatively predict (via perturbation of the excited states given by the four-orbital model) the shifts in the absorption spectrum and in the Raman lines sensitive to electronic structure. In particular, a knowledge of the response of Raman marker lines to such well-defined changes in electronic structure should make Raman data more useful as a probe of interactions between a metalloporphyrin and its environment. This is especially important for the iron–porphyrins for which interpretation of protein-dependent absorption spectral changes is made difficult by charge-transfer transitions in the region of the $\pi \rightarrow \pi^*$ bands. In addition, axial ligation in hemoproteins is more elaborate than for their copper-modified counterparts, for which the present results indicate only a change in σ-donation by the proximal histidine residue leading to core expansion that is sensed by the Raman core-size marker lines. Nevertheless, we now know the pattern of shifts in the Raman marker lines to be expected upon a change in ligand σ-donation alone is relatively larger shifts in the core-size lines than in the oxidation state marker line ν_4.

Recently, changes in the absorption spectrum associated with π–π aggregation have been found to be *quantitatively*

described by the exact relationships predicted by the four-orbital model for a series of metallouroporphyrins (Shelnutt, 1984). Similar spectral changes occur for the metalloprotoporphyrins (J. A. Shelnutt, unpublished results). As a result, a quantitative treatment of both π–π dimerization and axial ligand effects on the absorption spectra of ^{Cu}cyt-*c* is feasible. Preliminary analysis shows the following: (1) the qualitative arguments given here concerning the effect of axial ligation on the frontier orbitals are correct; (2) however, π–π dimerization affects the $\pi \rightarrow \pi^*$ transition dipoles (R_1 and R_2 in Figure 7), which have been assumed constant in the present analysis; (3) disaggregation, which we have ignored in the analysis described here, and axial ligation cause comparable reductions in the separation of the a_{1u} and a_{2u} orbitals.

Registry No. Cu(ProtoP), 14494-37-2; Cu(OEP), 14409-63-3; $[Cu(UroP)]_2$, 90990-73-1; Cu, 7440-50-8.

References

Abe, M., Kitagawa, T., & Kyogoku, Y. (1978) *J. Chem. Phys. 69*, 4526–4534.

Adar, F. (1975) *Arch. Biochem. Biophys. 170*, 644–650.

Adar, F. (1977) *Arch. Biochem. Biophys. 181*, 5–7.

Alston, K., & Storm, C. B. (1979) *Biochemistry 18*, 4292–4300.

Andres, S. F., & Atassi, M. Z. (1970) *Biochemistry 9*, 2268–2275.

Atassi, M. Z. (1967) *Biochem. J. 103*, 29–35.

Baker, E. W., Brookhart, M. S., & Corwin, A. H. (1964) *Inorg. Chem. 86*, 4587–4590.

Blumberg, W. E., & Peisach, J. (1965) *J. Biol. Chem. 240*, 870–876.

Chikira, M., Kon, H., Hawley, R. A., & Smith, K. M. (1979) *J. Chem. Soc., Dalton Trans.*, 245–249.

Chikira, M., Matsuura, S., & Kon, H. (1980) *Biochim. Biophys. Acta 622*, 105–114.

Choi, S., Spiro, T. G., Langry, K. C., & Smith, K. M. (1982) *J. Am. Chem. Soc. 104*, 4337–4344.

Dickinson, L. C., & Chien, J. C. W. (1974) *Biochem. Biophys. Res. Commun. 58*, 236–240.

Dickinson, L. C., & Chien, J. C. W. (1975) *Biochemistry 14*, 3526–3542.

Dixit, S. N., Waring, A. J., & Vanderkooi, J. M. (1981) *FEBS Lett. 125*, 86–88.

Dixit, B. P. S., Waring, A. J., Wells, K. O., III, Wong, P. S., Woodrow, G. V., III, & Vanderkooi, J. M. (1982) *Eur. J. Biochem. 126*, 1–9.

Falk, J. E. (1964) *Porphyrins and Metalloporphyrins*, p 76, American Elsevier, New York.

Findlay, M. C., Dickinson, L. C., & Chien, J. C. W. (1977) *J. Am. Chem. Soc. 99*, 5165–5173.

Flatmark, T., & Robinson, A. B. (1968) *Structure and Function of Cytochromes* (Okunuki, K., Kamen, M. D., & Sekuzu, I., Eds.) p 318, University Park Press, Baltimore, MD.

Gouterman, M. (1959) *J. Chem. Phys. 30*, 1139–1161.

Gouterman, M., Schwarz, F. P., Smith, P. D., & Dolphin, D. (1973) *J. Chem. Phys. 59*, 676–690.

Kashiwagi, H., & Obara, S. (1981) *Int. J. Quantum Chem. 20*, 843–859.

Kim, D., Holten, D., & Gouterman, M. (1984) *J. Am. Chem. Soc. 106*, 2793–2798.

Kitagawa, T., Ogoshi, H., Watanabe, E., & Yoshida, Z. (1975) *J. Phys. Chem. 79*, 2629–2635.

Moore, G. R., Williams, R. J. P., Chien, J. C. W., & Dickinson, L. C. (1980) *J. Inorg. Biochem. 12*, 1–15.

Perrin, M. H., Gouterman, M., & Perrin, C. L. (1969) *J. Chem. Phys. 50*, 4127–4139.

Perutz, M. (1970) *Nature (London) 228*, 726–734.

Petke, J. D., Maggiora, G. M., Shipman, L. L., & Christoffersen, R. E. (1978) *J. Mol. Spectrosc. 71*, 64–79.

Reynolds, A. H., Straub, K. D., & Rentzepis, P. M. (1982) *Biophys. J. 40*, 27–31.

Roos, B., & Sundbom, M. (1970) *J. Mol. Spectrosc. 36*, 8–14.

Satterlee, J. D., & Erman, J. E. (1983) *J. Biol. Chem. 258*, 1050–1056.

Shelnutt, J. A. (1981a) *J. Am. Chem. Soc. 103*, 4275–4277.

Shelnutt, J. A. (1981b) *J. Chem. Phys. 74*, 6644–6657.

Shelnutt, J. A. (1983a) *J. Phys. Chem. 87*, 605–616.

Shelnutt, J. A. (1983b) *J. Am. Chem. Soc. 105*, 774–778.

Shelnutt, J. A. (1983c) *Inorg. Chem. 22*, 2535–2544.

Shelnutt, J. A. (1984) *J. Phys. Chem.* (in press).

Shelnutt, J. A., & Dobry, M. M. (1983) *J. Phys. Chem. 87*, 3012–3015.

Shelnutt, J. A., & Ondrias, M. R. (1984) *Inorg. Chem. 23*, 1175–1177.

Shelnutt, J. A., O'Shea, D. C., Yu, N.-T., Cheung, L. D., & Felton, R. H. (1976) *J. Chem. Phys. 64*, 1156–1165.

Shelnutt, J. A., Rousseau, D. L., Dethmers, J. K., & Margoliash, E. (1979a) *Proc. Natl. Acad. Sci. U.S.A. 76*, 3865–3869.

Shelnutt, J. A., Rosseau, D. L., Friedman, J. M., & Simon, S. R. (1979b) *Proc. Natl. Acad. Sci. U.S.A. 76*, 4409–4413.

Shelnutt, J. A., Rousseau, D. L., Dethmers, J. K., & Margoliash, E. (1981) *Biochemistry 20*, 6485–6497.

Shelnutt, J. A., Satterlee, J. D., & Erman, J. E. (1983) *J. Biol. Chem. 258*, 2168–2173.

Shelnutt, J. A., Dobry, M. M., & Satterlee, J. D. (1984) *J. Phys. Chem.* (in press).

Smith, K. M. (1975) *Porphyrins and Metalloporphyrins* (Smith, K. M., Ed.) Appendix, Elsevier Scientific, Amsterdam.

Spaulding, L. D., Chang, C. C., Yu, N. T., & Felton, R. H. (1976) *J. Am. Chem. Soc. 97*, 2517–2525.

Spellane, P. J., Gouterman, M., Antipas, A., Kim, S., & Liu, Y. C. (1980) *Inorg. Chem. 19*, 386–391.

Spiro, T. G. (1982) in *Iron Porphyrins* (Lever, A. B. P., & Gray, H. B., Eds.) Part II, Chapter 3, Addison-Wesley, Reading, MA.

Spiro, T. G., & Strekas, T. C. (1974) *J. Am. Chem. Soc. 96*, 338–345.

Spiro, T. G., & Burke, J. M. (1976) *J. Am. Chem. Soc. 98*, 5482–5489.

Spiro, T. G., Stong, J. D., & Stein, P. (1979) *J. Am. Chem. Soc. 101*, 2648–2655.

Straub, K. D., & Rentzepis, P. M. (1983) *Biophys. J. 41*, 411a.

Turner, S. R. (1971) Ph.D. Thesis, Duke University, Durham, NC.